14

Measurement of Levitation Forces in High Temperature Superconductors

İbrahim Karaca
Department of Physics, Niğde University, Niğde
Turkey

1. Introduction

Magnetic Levitation (MagLev) has become a popular of new technological applications since the discovery of the new superconductor materials, in 1987. MagLev transportation systems have been ignited the human's imagination about levitated motion. MagLev systems have become very important in the transportation and other applications in the future life in the world is generally based on the superconductor technology. These applications are ranging from in an energy efficient prototype of a cryogen transfer line to in space energy storage systems.

The superconducting behaviors of materials originated from two basic physical properties. One of them is disappearance of the electrical resistance below the transition temperature (T_C) in the superconducting materials. The another of them is special magnetic properties in an applied magnetic field (H) including perfect diamagnetism at low fields (low temperature superconductors (LTS) and high temperature superconductors (HTSs)) and the penetration of quantized magnetic flux (vortices or flux lines) at higher fields regions (HTSs). The electrons in the superconducting state can be described by a macroscopic wave function which is undisturbed by scattering and, in the absence of applied fields and currents, uniform in space over macroscopic distances. This coherence of the superconducting state is preserved even in the presence of weak currents and magnetic fields (below the upper critical field (H_{C2}), which is a necessary condition for the practical use of the high temperatures superconductors (HTSs) in strong magnetic fields. The additional condition for new applications in these superconductors materials have been used to avoid any motion of flux lines. This can be achieved through the introduction of pinning centers in the superconductor, interacting, in most cases, with the normal conducting core of the flux lines. A flux line is composed of a normal conducting core regions and a surrounding circulating supercurrents area where the magnetic field and supercurrents fall off within penetration depth. The critical current density (J_C) increases with the applied magnetic field (H) increases and penetration depth (λ) decreases. The force-distance (permanent magnets and superconductor) hysteresis loops during the descending and ascending process expanded with critical current density increases.

The mechanism of superconductivity in high temperature superconductor (HTS) is still controversially discussed. The Bardeen-Cooper-Schrieffer (BCS) concept of a macroscopic quantum state of Cooper pairs remains the common basis in almost all theories proposed for HTS. However, there is no consensus about the origin of the pairing so far. The lack of an isotope effect in HTS of highest T_C would favor a non-phonon pairing mechanism as, for instance, d-wave pairing, whereas its presence in several HTS with lower T_C suggests a phonon-mediated s-wave pairing. The most experimental features favor d-wave pairing. A direct test of the phonon mechanism for pairing in HTSs is to check the sign change in the energy gap $(\Delta E_g(k))$ as function of momentum $(\hbar k)$. A d-state energy gap is composed of two pairs of positive and negative leaves forming a four-leaf clover. In contrast, the magnitude of an s-state may be anisotropic but always remains positive.

2. Levitation with superconductors

Superconducting levitation by using the permanent magnet (PM) is a fascinating property of the magnetic behavior of these materials. It can be mainly defined in two regimes for HTSs. In the first regime, the magnetic induction applied an external magnetic field to samples are expelled from the superconductor and do not penetrate inside of the superconductor materials, which is defined as Meissner effect. This effect is possible only if the applied magnetic field does not exceed the first critical field (so called H_{C1}) of the HTS. To obtain experimentally levitation in the Meissner state, it is convenient to close the magnet very carefully, after cooling the superconductor. In the second regime of the levitation, i.e., the mixed state, a vortex penetration through for HTSs, occurs only for fields between the first (H_{C1}) and the second critical magnetic field (H_{C2}) of the HTSs. This is so because magnetic lines could be pinned if they penetrate in the sample and the superconductor would be switched to the mixed state. It is clearly that the levitation measurement is finding in the mixed state acceptable. Magnetic levitation effects are seen Meissner states as the same in HTSs and LTSs. But, magnetic levitation effects originated from flux lines for only HTSs.

When a superconductor is in the presence of a changing applied magnetic field, supercurrents (I_C) are induced inside the sample producing a diamagnetic response of the material. The interaction of the supercurrents with an inhomogeneous magnetic field can produce stable levitation. The flux lines in the small currents densities ($J < J_C$ for a certain critical current J_C) for the real HTSs can be pinned by inhomogenities. Under this condition, when an external applied field increases or decreases, the magnetic flux moves within the superconductor towards its interior or exterior until a critical slope is reached in the flux profile. The current density in this critical state attains its maximum value J_C. The critical slope behavior has been modeled by Bean's critical-state model and its extensions, phenomenological. Brandt showed qualitatively how from the pinning of flux lines some properties of levitation of HTSs can be explained in detail (Brandt, 1998).

Moon *et al.* measured the vertical forces on a levitating superconductor showing some of the main properties (Moon, 1988). This measurement has been extended by several groups in order to study the influence of orientation, material, or shape of superconducting samples, comparing, sometimes, thin films with bulk samples (Navau & Sanchez, 1998). On the other hand, a few models have been developed, most of them studying the interaction between a superconductor and a permanent magnet. Hellman *et al.* and Yang presented models based on total flux exclusion of the samples that thus describe the behavior of LTSs or HTSs materials with higher critical current densities (Navau & Sanchez, 1998). Schönhuber and Moon, Chan *et al.*, and Torng and Chen have taken into account the penetration of supercurrents, the latter with an applied field provided by a pair of oppositely wound coils (Schonhuber & Moon, 1994; Chan, *et al.,* 1994; Torng & Chen, 1992). Some papers have considered granular structure for the superconductors when grains are completely penetrated (Johansen, *et al.*, 1994; Riise, *et al.,* 1994).

All over the models mentioned above assume that a superconducting sample is small enough to consider the magnetic field gradient constant along it. Demagnetization field of the sample due to the finite dimensions of the HTSs has been neglected by the same time. Demagnetization effects have been take into only account in theoretical calculation so far Tsuchimoto *et al.* have calculated the dependence of levitation force upon different geometrical parameters of a PM-HTSs system by using the an axisymmetric boundary element analysis (Tsuchimoto, *et al.,*1994). Portabella *et al.* have been used finite element calculations for the levitation force-distance $(F-x)$ hysteresis loop in order to estimate the value of critical current of a HTSs. Navau and Sanchez calculated the dependence of maximum vertical force upon the length of superconductor, considering both the demagnetization effect and the nonuniformity of the field gradient. In spite of these efforts, a systematic treatment of vertical levitation force for which the applied magnetic field can not be assumed to have a constant gradient has not been developed yet. In the scope of this chapter, we have been observed vertical levitation force as a function of distance between PM and HTSs. Moreover, most of the developments consider the superconductor to be in the critical state and describe it by means of Bean's critical-state model considering the critical current (J_C) as constant.

The most HTSs present a dependence of their critical current density (J_C) upon the internal magnetic field. Some analytical expressions have been proposed and successfully applied to describe the magnetic properties of superconductors (Navau & Sanchez, 1998). Therefore it is necessary to include such dependence in the study of the levitation behavior of the HTSs.

Kim's model dependence on the critical current density was developed by Tsuchimoto *et al.* with numerical (Navau & Sanchez, 1998). But, physical properties dependence on critical current density (J_C) in levitation behavior has not been studied in general so far.

To obtain critical current density (J_C), the consideration includes:

i. Character of response to applied field, equations of dependence on properties of materials;
ii. History of applied field;
iii. The initial state of the system;
iv. The boundary conditions.

Models on magnetization of the HTSs as can be seen in below.

a. Bean model,

Bean proposed a so-called critical-state model in which the hysteresis loop is plugged in a macroscopic parameter critical current density J_C (Bean, 1964). According to the Bean model, critical current density J_C presumes a constant and given as

$$J_C(H_i,T) = J_C(T) \tag{1}$$

where H_i and T are the local magnetic field and the temperature with respectively. In the model also pointed out that J_C was directly determined by the microstructure of the superconductors. The relationship of J_C versus temperature can be expressed as $J_C(T) = J_{C0}(T_C - T) / (T_C - T_0)$ (Berger, *et al.* 2007), where T_C is the critical temperature and J_{C0} the critical current density according to the reference temperature (T_0).

b. Kim model,

Anderson and Kim modified the Bean model (Anderson & Kim, 1964; Kim, et al. 1962) and J_C was suggested that it should vary with the local magnetic field and should have the form

$$J_C(H_i,T) = \frac{J_C(T)}{1 + H_i / H_0} \tag{2}$$

where H_0 is a macroscopic materials parameter with the dimension of field. The model was found to fit the experimental results for some conventional superconductors for a solid cylinder shaped superconductors.

According to Kim model the J_C depend on the term H_i / H_0, which may vary considerably among different materials. Watson showed that, for some systems, the condition $H_i >> H_0$ is fulfilled. Eq. (2) shows a simple linear field dependence of J_C, $J_C(H_i) = A - CH_i$, where A and C are constants (Hindley & Watson, 1969).

c. Power law model,

Irie and Yamafuji are focus on the specific pinning mechanisms, a power-law field dependence of J_C was suggested (Irie & Yamafuji, 1967),

$$J_C(H_i,T) = \frac{K(T)}{H_i^n} \tag{3}$$

where K is a materials parameter and n directly reflects pinning strength. An empirical formula based on experimental results developed by Fietz et al. (Fietz, *et al.*, 1964),

$$J_C(H_i,T) = J_C(T)\exp\,(-H_i / H_0)\,. \tag{4}$$

A general critical-state model was developed for the critical current density. It is obtained from Eq. (1-4) as the next form,

$$J_C(H_i,T)=\frac{J_C(T)}{\left[1+H_i\,/\,H_0(T)\right]^{\beta}} \tag{5}$$

where β is a dimensionless constant. Eq. (5) can be converted to Bean and Kim models by using the Eqs. (1) and (2), respectively if the $\beta = 0$ and 1. Eq. (3) is obtained when the condition $-H_i / H_0 >> 1$ is satisfied in eq. (5) and the K and n are set to $J_C(T) = \mathrm{H}_0^{\beta}$ and β, respectively (Xu, et al., 1990). In the conditions of $-H_i / H_0 << 1$ and $\beta >> 1$, with $H_0 / \beta << \mathrm{H}_0$, where H_0 is a finite value with dimension of field, and taking the limit of $J_C(H_i)$ with the preceding conditions and letting $-H_i / H_0 = x$, it has

$$\lim J_C(H_i,T)=\frac{J_C(T)}{\lim\limits_{x\to 0}\left[1+x\right]^{\beta}}=\frac{J_C(T)}{\lim\limits_{x\to 0}\left[1+x\right]^{(1/x)(H_0/H_0)}}=J_C(T)\exp(-H_i\,/\,H_0) \tag{6}$$

It can be seen that Eq. (6) has the same form as Eq. (4) and that their physical meanings are identical.

d. Yin model,

Material's equation, known as Yin model, has been developed in the form as (Yin *et al.*, 1994),

$$E(J)=2\upsilon_0 H\exp\left[-\left(\frac{U_0+W_V}{kT}\right)\right]\sinh\left[\frac{W_L}{kT}\right] \tag{7}$$

Where υ_0, U_0, $W_V = \eta\upsilon P = E(J)HP/\rho_f$, $W_L = JHP$ and P are a prefactor with dimension of velocity, the pinning potential, the viscous dissipation term of flux motion with viscosity coefficient (with $\eta = HH_{C2}/\rho_n = H^2/\rho_f$), the energy due to Lorentz driving force, a product of the volume of the moving flux bundle and the range of the force action, respectively. In the υ term in the W_V corresponds to $\upsilon_0\exp\left[-U(J)/kT\right]$. U represents the activation barrier. Yin model includes pinning barrier term, viscous dissipation term and direction dependent. It provides a unified description which covers all regimes of flux motion: thermally activated flux flow, flux creep, critical state and flux flow. Yin model contain Anderson–Kim model, Bardeen–Steven model and critical state model $(\vec{F}_P = \vec{J}_C \times \vec{H})$ as its specific forms (Yin *et al.*, 1994).

There are different ways of calculation of magnetic field (H_{PM}) of permanent magnets (Moon, 1990; Sanchez & Navau, 2001; Brandt, 1990; De Medeiros, *et al.* 1998),

i. Biot–Savart's law: Calculating B_{PM} with Biot–Savart's law.

ii. Scalar potential method: Calculating scalar potential φ_μ in current-free area, H_{PM} is the gradient of φ_μ.

iii. Vector potential method: Calculating vector potential $A(PM)$, H is the curl of A.

Field expression in cylindrical coordinates (John David Jackson, 1998), is

$$\vec{H}(\vec{r}) = \vec{\nabla} \times \vec{A} = \frac{\mu_0}{4\pi} \int\int\int_V \frac{\vec{J}(\vec{r}) \times (\vec{r} - \vec{r}\,')}{|\vec{r} - \vec{r}\,'|} dv' \tag{8}$$

Numerical methods have been developed towards to solve the $J_C(H)$ and the levitation force. Analysis and simulation can be carried out based on above models and various parameters.

The levitation forces evaluation of distance between HTS and PM (or air gap) are seen in Fig. 1. As can be seen from this figure, levitation forces in a magnetic media for experimental and theoretical calculation decreases when distance between HTS and PM increases.

There are several methods for the calculation of levitation force in magnetic field. Some of these methods are Lorentz force equation (Chun &Lee, 2002), Maxwell's stress tensor (Amrhein & Krein, 2009) and virtual work methods (Vandevelde& Melkebeek, 2001). The Lorentz force equation method is important to know the exact distribution of the critical current density and the magnetic field. The Maxwell's stress tensor method is calculated by the integration of the Maxwell's stress tensor on an arbitrary surface surrounding the object.

The magnetic force as the virtual work method is given by the derivation of the co-energy with respect to a virtual displacement.

The magnetic levitation forces evolution of the distance of between HTS and PM with experimental and different theoretical models are seen in Fig. 1.

From this figure, levitation force nearly exponentially increase while distance of between HTS and PM decreases. But, the experimental results nearly agree with the Lorentz force equation methods. In other words, from the comparison, the result by the Lorentz force methods is in strict correspondence with the experimental results quantitatively according to the others simulation methods. Agreement between the Lorentz force methods with the experimental results originated perhaps from the penetration of the applied field into HTSs. Because of the penetration of the applied field into the HTS occurs where the vortex state is. This field passes through the HTSs produce a flux tubes. This states in this type studied so called known repulsive magnetic field in general. Finally, compatible Lorentz force method with the experimental result is not surprising.

Since the discovery of high temperature superconductors (HTSs) this interaction has achieved considerable attention, mainly due to its capability of producing stable non-contacting conditions for such (HTS-PM) systems. The magnetic levitation forces can be demonstrated very easily in experimentally. But, their theoretical models are far more difficult. The reason for these difficulties are the below.

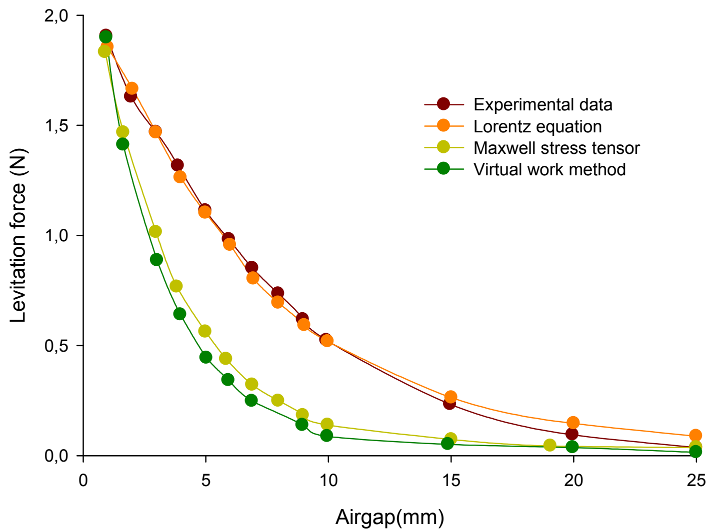

Fig. 1. The levitation forces evolution of the distance of between HTS and PM with experimental and different theoretical models (Chun & Lee, 2002).

1. The HTS's are of HTS with a strongly irreversible magnetic behavior, i.e., their magnetization depends on the prehistory of the external magnetic fields.
2. The levitation phenomenon between HTS and PM materials has been studied for magnetic granularity or polycrystalline bulk materials in general. The magnetic levitation force studies are very poor for single crystalline materials.
3. A finite levitation force is required non uniform magnetic field.

During the past years, many research groups have done extensive studies of levitation forces using HTS bulk materials of various kinds (Takao *et al.* 2011; Lu *et al.*, 2011; Krabbes *et al.*, 2000). The higher levitation force and stable levitation or suspension between a PM and a bulk superconductor, makes superconducting bulks possible for various applications such as superconducting magnetic bearings, flywheel, magnetic levitation transportation systems, generators or motors and permanent magnets.

3. Levitation experimental system and data analaysis

The levitation forces measure between permanent magnet and superconducting high temperature, bulk or film in general. The critical current has the crucial role in the levitation force measuring system. The levitation force between HTS and PM originated from by the interaction between the induced electric current in the HTS and the magnetic field from the PM. The critical current density $J_C(H)$ is closely related with the flux pinning center density and flux pinning force of the sample, and also closely related with the flux pinning, depinning process and the magnetic flux creep rate during the levitation force measurement. The $J_C(H)$ is also a fixed parameter (if we consider the process based on

Bean's model) because the sample is the same, so the levitation force is only related with the total induced electric current in the sample which is depending on magnet moving speed, this is the only variable during the measurement. Superconductors is different from perfect conductor, that if a superconductor is cooled below certain temperature (is called critical temperature, T_C) and an external magnetic field is applied then the superconductor repel the magnetic field because of the supercurrent. This super-current is made of the inside the superconductor via of the induced of the external field as the same Lenz law. This situation, the superconductor has the supercurrent as defined superconductor. Firstly grains effected and a current circulate interior of the grain, which is called internor current, I_C . Secondly all of the interior current sums to surface of the superconductor and they called screening current, I_S ; which is repulsive and screening to external magnetic field.

The screening currents produce a mutually repulsing behavior, so the external magnetic field do not penetrate interior of the superconductor, which is called Meissner effect in the superconductor. The German physicists Meissner and Ochsenfeld discovered the phenomenon in 1933 by measuring the magnetic field distribution outside superconducting thin and lead samples. These samples, in the presence of an applied magnetic field, were cooled below what is called their superconducting transition temperature. Below the transition temperature the samples canceled nearly all magnetic fields inside. They detected this effect only indirectly; because the magnetic flux is conserved by a superconductor, when the interior field decreased the exterior field increased. The experiment demonstrated for the first time that superconductors were more than just perfect conductors and provided a uniquely defining property of the superconducting state.

Macroscopic transport properties mechanism of the grain boundary effect on HTS is not entirely understood yet, though on this mechanism several theoretical models have been suggested (Luine & Kresin, 1998; Coble, 2009). In particular, it is assumed that the grain boundary effects are describing as that to following factors: (i) a decrease of electron free path in vicinities of grain boundaries; (ii) stress-field-induced structural disorder and pinnig of magnetron vortices at grain boundaries; (iii) formation of the antiferromagnetic phase within grain cores; (iv) faceting of grain boundaries and d-symmetry of the superconducting order parameter, (v) deviations from bulk stoichiometry in vicinities of grain boundaries.

Figures 2-3 shows a schematic representation of the preparing of the HTS sample with a wet-technique (or ammonium nitrate method) and annealing process of the HTS disk, respectively. The starting material was the powder of nominal $Bi_{1.84}Pb_{0.34}Sr_{1.91}Ca_{2.03}Cu_{3.06}O_{10}$ compound, which was synthesized by a wet-technique using high-purity (>99.99%) Bi_2O_3, PbO, $SrCO_3$, $CaCO_3$ and CuO, We produce our powder by using this method at room temperature. Then, the powder was calcined at 700 ˚C for 10h, twice as much, and pressed into pellets with 225 MPa. The pellets were placed in a preheated furnace at 850 ˚C for 100 h then directly cooled to room temperature for quench. After this sintering process pellets regrinding and the powders at various pressures and time were pressed in to cylindrical superconductor disk (CSD: $Bi_{1.84}Pb_{0.34}Sr_{1.91}Ca_{2.03}Cu_{3.06}O_{10}$) with diameter ($2r$) of 13 mm and height (h) of 13.52 mm. The CSD was placed in a preheated furnace at 815 ˚C at a rate of 0.1 ˚C/min for 100 h then directly cooled to room temperature. The details of producing of HTS material was given in previously our work (Karaca, 2009).

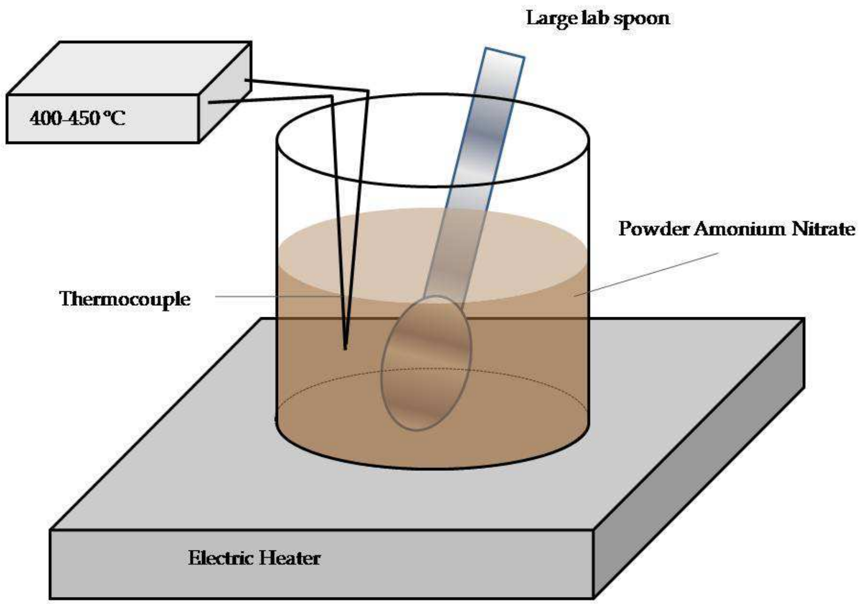

Fig. 2. Schematic representation of the preparing of HTS sample.

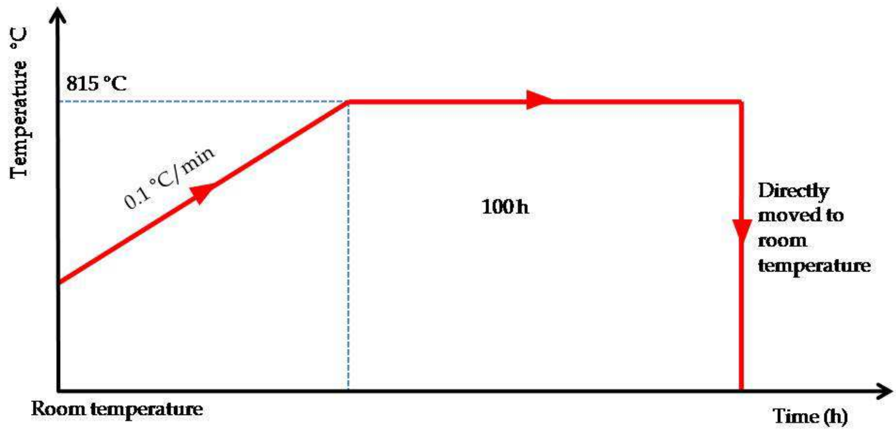

Fig. 3. Schematic representation of the annealing process of the HTS disk.

Magnetic properties were measured by using the magnetic levitation force-distance (between HTS and PM) system at the temperature 77 K in Fig. 4. Measurements were performed in the zero field cooled (ZFC) regimes in applied magnetic field $H_r = 0.15T$.

Magnetic repulsive and attractive forces between the HTS disk and PM were measured using a homemade levitation measuring device (Fig.4). It is figure out in Fig.4 an Nd–B–Fe permanent magnet (1.6x1.4x0.34 cm^3 and $H_r = 0.15T$) was put on the plate of a sensitive electronic scale. CSD sample (13 mm in diameter) was immobilized at the bottom of a liquid nitrogen-filled receptacle which is movable in the vertical direction (CSD and PM are symmetrically fixed on the same line). This receptacle was then placed just above the plate of the balance without touching it. Thus, the observed weight change of the magnet directly reflected the magnetic force induced in this handmade system (Benlhachemi, *et al.*, 1993, Karaca, 2009).

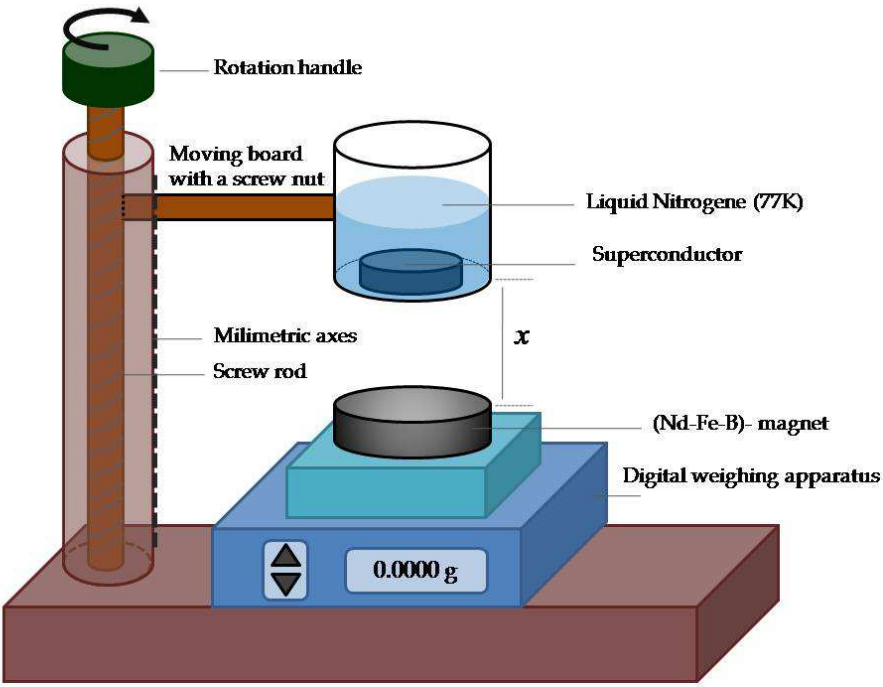

Fig. 4. Schematic representation of the magnetic levitation force-distance (between HTS and PM) hysteresis loop measurement experimental system.

The magnetic levitation force-distance (between HTS and PM) $(F-x)$ hysteresis loop ZFC process during the descending and ascending process is seen in Fig.5. Similarly, the full light green and full dark green circles correspond to the levitation force curves ascending and descending with respectively. The hysteresis curves of magnetic levitation are not the same. In other words, magnetic levitation force when distance ascending faster than magnetic levitation force while distance descending. However, the hysteresis loops strongly depend on the size of grains and their connectivity in the bulk HTS. The magnetic levitation forces nearly the same when distance increases from 20 mm to 36 mm. this behavior corresponds to Meissner effects. The levitation force linearly decreases when distance increases from 0 mm to 6 mm. The external magnetic field fully penetrated HTS disk in this space (0-6 mm), because, there are no hysteretic behavior in this area. The maximum hysteretic phenomena are seen in the distance range 6-20 mm. This phenomena attributed that the vortex state. The results of the levitation force have generally been measured in a ZFC process, a few works were done in the field cooled (FC) process (Yang *et al.*,2003)**.**

The force between HTS and PM system can be written as $F = \mu(dH/dx)$. Here, μ is the magnetic moment related with the bulk magnetization $\vec{M}$ $\left(\vec{M} = \sum_{i=1}^{n} \vec{\mu}_i\right)$. dH/dx is the field gradient produced by the magnet. The trapped field in HTS originated from the PM, an attractive force occurs when the sample is moved away from the PM. This result can be attributed to the number of pinning centers in the HTS sample, which results in an increase of trapped magnetic field inside the samples. In addition, the levitation force is related to the grain size and crystallographic orientation.

The force-distance $(F-x)$ between CSD ($Bi_{1.84}Pb_{0.34}Sr_{1.91}Ca_{2.03}Cu_{3.06}O_{10}$) and PM always hysteresis loop as an example for this chapter during the descending and ascending process are seen in Fig. 5.

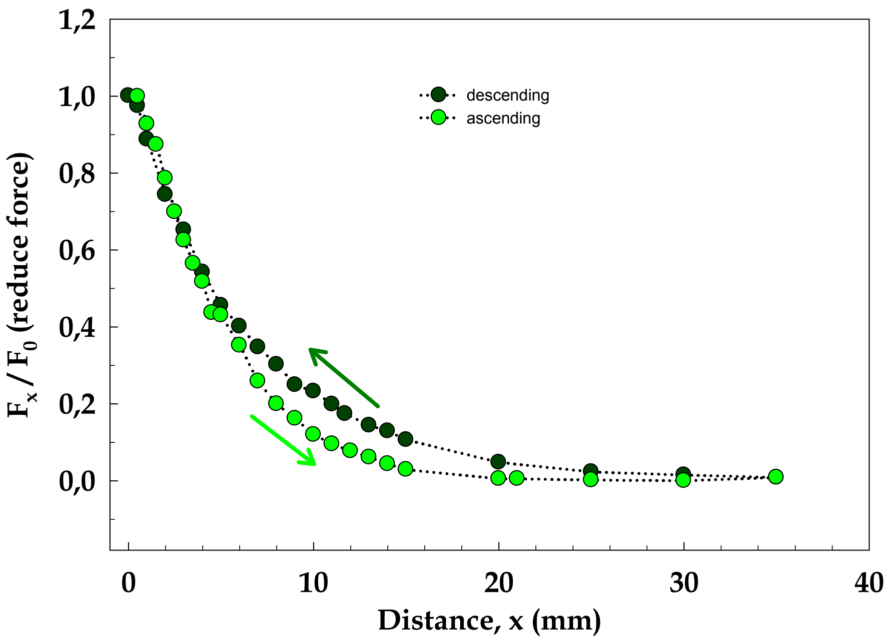

Fig. 5. The interaction force between a CSD and a PM always shows a force-distance ($F-x$) hysteresis loop during the descending (dark green full circle) and ascending (light green full circle) process.

As can be seen from Fig.5, the levitation force while distance increasing smaller than levitation force while distance decreasing. The maximum values between of two levitation forces are seen near the 10 mm. These values are smaller than expectation values for HTS.

The levitation force can be related from the interaction between CSD and PM materials in general. This interaction between CSD and PM are mainly dependent on the properties of the CSD and the magnetic field distribution of the magnet. For a bulk superconductor, the levitation force is dependent on many parameters, such as the critical current density and grain radius, grain-orientation, thickness of the sample, and the cooling temperature. For a magnet, the levitation force is closely related with the magnetic flux density, magnetic field distribution, etc. But for a given pair of bulk superconductor and PM, it is known that the same levitation force can be obtained at a gap distance between the superconductor and the magnet, because of the magnetization history of the superconductor, by a mechanical descending and ascending process of the magnet during the axial levitation force measurement state (Yang *et al.,* 2003).

The low levitation force of sintered superconductor materials can be attributed to two intrinsic material problems of a superconductor in this chapter (Murakami, 1993). The first is the grain boundary weak-link problem and the second is the weak flux pinning problem. In order to resolve these two problems, different material processing techniques have been developed from other workers (Chen *et al.,* 1998).

4. Technological applications of levitation forces in HTS

Temperatures in the range near the 4-30 K and near the 30-180 K are called the low temperature superconductors (LTS) and high temperature superconductors (HTS) regime with respectively. In the scope of this chapter, we have studied levitation force-distance loops for HTS in 77 K. In the recent 30 years, LTS and especially HTS are in a class of superconductor. HTS structures have potential applications in a broad range topical areas, superconducting magnetic energy storage (SMES), power devices including transmission cable, HTS motors and HTS generators, superconducting fault current limiters (SFCL), and high field magnets. See the Fig.6 in below for an example of some application of these type HTS samples.

Fig. 6. Some application of the HTS (www.superpower-inc.com; http://yahoo.brand.edgar-online.com).

The levitation force hysteretic loops applied to new technologies as medical and space technologies in general.

HTS generators are substantially smaller and lighter than copper based machines. These advantages are very attractive in a ship environment. HTS power cables will enable utilities to upgrade power density by 2 to 8 times power corridors because HTS cables transmit power with essential no electrical resistance. Superpower's SFCL technology is enable scaling to high voltage and current with customization to the user's requirements, losses or voltage drop across the device during normal operation, and etc. The HTS technology can be used to make all superconducting magnets with field that will soon exceed 30 Tesla (see for detail, www.superpower-inc.com).

5. Summary

In the scope of this chapter, we have focus on the magnetic levitation force-distance loops for HTS samples. The inter CSD and PM exchange type interaction are determined magnetic levitation forces. The magnetic levitation forces are heavily dependence on grain size, grain connectivity, critical current density, history of applied magnetic field and etc. Combination with hysteresis $(F-x)$ results, these indicate that the Meissner effects, vortex state and metallic behavior are seen the same. The CSD with ZFC process showed that the sample has low quality with weak-link characteristics. A typical hysteresis loop of the axial levitation force between the permanent magnet and the CSCD showed the lower repulsive force in this chapter. This phenomenon is attributed to the fact that the wet technique causes the production of lower dense samples, and is caused by a lower critical current density (Altunbaş et al., 1994; Karaca et al., 1998) and by a lower levitation force. It is considered that the changes in the levitation force are related to the grain orientation, the homogeneity, and the number of the pinning centers in the samples (Yanmaz et al., 2002). Levitation force measurements need to investigate several factors end different materials. In the future life will be need to this investigation results.

6. Acknowledgements

I would like to thanks Mehmet Ali Güzel for help.

7. References

Abrikosov, A. A. (1957). *Zh. Eksp. Teor. Fiz.*, Vol.32, pp. 1442.

Alamgir, A. K., Yamada, M. H., Harada, N., Osaki, K. & Tada, N. (1999). *IEEE Transaction on Appl. Supercond.*, Vol.9, pp. 1864.

Altunbaş, M., Yanmaz, E., Nezir, S., Karal H. & Vidadi Yu A. (1994). *J. Alloys and Compounds*, Vol.215, pp. 263.

Altunbaş, M., Yanmaz, E., Nezir, S., Karal, H. & Vidadi Yu A. (1994). *J. Alloys and Compounds*, Vol.215, pp. 263

Amrhein, M., Krein, P.T. (2009). Force Calculation in 3-D Magnetic Equivalent Circuit Networks With a Maxwell Stress Tensor", *Energy Conversion, IEEE Transactions on,* Vol.24 Issue: 3, pp. 587 – 593.

Anderson, P. W. & Kim, Y. B. (1964). Hard superconductivity: theory of the motion of abrikosov flux lines, *Rev. Mod. Phys.*, Vol. 36, No. 1, pp. 3943.

Bean, C. P. (1962). *Phys. Rev. Lett.,* Vol.8, pp. 250.

Bean, C. P. (1964). Magnetization of high-field superconductors, *Rev. Mod. Phys.*, Vol.36, No. 1, pp. 31-39.

Benlhachemi, A., Golec S. & Gavarri, J.R. (1993). *Physica C: Superconductivity*, Vol.209, pp. 353.

Berger, K., Lévêque, J., Netter, D., Douine, B., & Rezzoug, A. (2007). Influence of temperature and/or field dependences of the E-J power law on trapped magnetic field in bulk YBaCuO, *IEEE Trans. Appl. Super.*, Vol. 17, No. 2, pp. 3028-3031.

Brandt, E. H. (1990). *Appl. Phys. Lett.*, Vol.53, pp. 1554.

Brandt, E.H. (1998). Superconductor Disks and Cylinders in Axial Magnetic Field: I. Flux Penetration and Magnetization Curves, *Phys. Rev. B*, Vol.58, pp. 6506-6522.

Chan, W. C., Jwo, D. S., Lin, Y. F. & Huang, Y. (1994). Magnetic levitation of $YBa_2Cu_3O_y$ single crystals, *Physica C: Superconductivity* Vol.230, pp. 349-353.

Chen, I.G., Hsu, J.C., Janm, G., Kuo, C.C., Liu, H.J., & Wu, M. K. (1998). *Chin. J. Phys.*, Vol.36, pp. 420.

Chun,Y.D. & Lee,J. (2002). Comparison of magnetic levitation force between a permanent magnet and a high temperature superconductorusing different force calculation methods, *Physica C,* Vol.372–376, pp. 1491–1494.

Coble, R. L. (2009). Sintering Crystalline Solids. I. Intermediate and Final State Diffusion Models, *Journal of Applied Physics,* Vol.32 Issue:5, pp. 787 – 792.

Davis, L. C. (1990). *J. Appl. Phys.*, Vol.67, pp. 2631.

De Medeiros, L.H., Reyne G., Meunier, G. (1999). *IEEE Transactions on Magnetics*, Vol.34 (5), pp. 3560–3563.

De Medeiros, L.H., Reyne, G., Meunier, G. (1998). Comparison of Global Force Calculations on Permanent Magnets, *IEEE Transactions On Magnetics*, Vol. 34, No. *5.*

De La Cruz, A., Badía, A. (2002). *Physica B: Physics of Condensed Matter*, Vol.321, Issue 1-4, pp. 356-359. DOI: 10.1016/S0921-4526(02)01074-8.

Essmann, U. & Truble, H. (1967). *Phys. Lett. A,* Vol.24, pp. 526.

Fietz, W. A., Beasley, M. R., Silcox, J., & Webb, W. W. (1964). Magnetization of superconducting Nb-25%Zr wire, *Phys. Rev.*, Vol.136, No. 2A, pp. A355-A345.

Gao, W. & Sande, J. B. V. (1992). *Supercond. Sci. Technol.*, Vol.5, pp. 318.

Hellman, F., Gyorgy, E. M., Johnson, D. W., Jr., O'Bryan, H. M., & Sherwood, R. C. (1988). *J. Appl. Phys*. Vol.63, pp. 477.

Hindley, N. K. & Watson, J. H., (1969). Superconducting metals in porous glass as granular superconductors, *Phys. Rev.,* Vol.183, No. 2, pp. 525528.

http://sciyo.com/articles/show/title/wind-power-integrating-wind-turbine-generators-wtg-s-with-energy-storage

http://www.superpower-inc.com (2012)

http://yahoo.brand.edgar-online.com (2012)

Irie, F. & Yamafuji, K. (1967). Theory of flux motion in non-ideal type-II superconductors, *J.Phys, Soc. Jpn.*, Vol. 23, pp. 255-268.

J. Mizia, K. Adamiak, A.R. Eastham, G.E. (1988). *IEEE Transactions on Magnetics* Vol.24 (1), pp. 447–450.

Jin, J. X. (2006). High Tc superconductor theoretical models and electromagnetic flux characteristics, *Journal of Electronic Science and Technology of China,* Vol. 4, No. 3, pp. 202-208.

Jin, J. X., Zheng, Lu H. (2007). *Physica C: Superconductivity*, Volumes 460-462, Part 2, pp. 1457-1458 DOI:10.1016/j.physc.2007.04.151.
Johansen, T. H., & Bratsberg, H. (1993). *J. Appl. Phys.*, Vol.74, pp. 4060.
Johansen, T. H., Bratsberg, H., Riise, A. B., Mestl, H. & Skjeltorp, A. T. (1994). *Appl. Suppercond*. Vol.2, pp. 535.
Johansen, T. H., Yang, Z. J., Bratsberg, H., Helgesen, G., & Skjeltorp, A. T. (1991). *Appl. Phys.Lett.* Vol.58, pp. 179.
Jones, T. E., Mc Ginnis, W. C., Jacobs, E. W., Bossp, R. D., Thibbado, M., Briggs, J. S., & Glad, W. E. (1994). *Physica C*, Vol.201, pp. 279.
Karaca, I. (2009). Characterization of a Cylindrical Superconductor Disk Prepared by the Wet Technique with Microstructure Analysis and Levitation Force Measurements Using a PermanentMagnet, *Chinese journal of Physics,* Vol. 47, No.5, pp. 690-696.
Karaca, I., Celebi, S., Varilci, A. & Malik, A. I. (2003). *Supercond. Sci. Technol*., Vol.16, pp. 100.
Karaca, I., Ozturk, A., & Nezir, S. (1998). *J. Alloys and Compounds* Vol.268, pp. 256.
Kim, Y.B., Hempstead, C. F. & Strnad, A. R. (1962). Critical persistent currents in hard superconductors, *Phys. Rev. Lett.,* Vol. 9, No. 7, pp. 306-309.
Krabbes, G., Fuchs, G., Schaatzle, P., Gruß, S., Park, J.W., Hardinghaus, F., Stover, G., Hayn, R., Drechsler, S.-L., Fahr, T. (2000). Zn doping of YBa Cu O in melt textured materials: peak effect 2 3 7 and high trapped fields, *Physica C*, Vol.330, pp. 181–190.
Liu, W., Wang, J. S., Liao, X. L., Zheng, S. J., Ma, G. T., Zheng, J., Wang, S. Y. (2010). *Physica C,* Vol.471, Issue 5-6, pp. 156-162. DOI: 10.1016/j.physc.2010.12.016
Lu, Y., Bai X., Ge, Y., Wang, J. (2011). Influence of Thickness on the Levitation Force of High-*Tc* Bulk over a Permanent Magnetic Guideway with Numerical Method, *J Supercond Nov Magn,* Vol.24, pp. 1967–1970.
Luine, J. A. & Kresin, V. Z. (1998). Critical current in high T_c grain boundary junctions, *J. Appl. Phys.* Vol. 84, pp. 3972, DOI:10.1063/1.368576.
Meissner, W., Ochsenfeld, R. (1933). *Naturwissenschaften,* Vol.21 (44), pp. 787–788.
Moon, F. C. (1990). *Int. J. Appl. Electromagn. Mater.* Vol.1, pp. 29.
Moon, F. C., Yanoviak, M. M. & Raj, R. (1988). *Appl. Phys. Lett.,* Vol.52, pp. 1534.
Murakami, M. (1993). *Appl. Supercond.,* Vol.1, pp. 1157.
Navau, C. & Sanchez, A. (1998). *Phys. Rev. B.* Vol.58, pp. 963–970, DOI:10.1103/PhysRevB.58.963.
Qin, M.J., Li, G., Liu, H.K., Dou, S.X. & Brandt, E.H. (2002). *Phys. Rev. B*, Vol.66 , pp. 024516.
Ren, H.T., Xiao, L., Jiao, Y.L., Zheng, M.H. & Chen, Y.X. (2003). *Chin. J. Low Temp. Phys.*, Vol.25 (1), pp. 11.
Riise, A. B., Johansen, T. H. & Bratsberg, H. (1994). The vertical magnetic force and stiffness between a cylindrical magnet and a high-T_c superconductor, *Physica C.*, Vol.234, pp. 108-114.
Riise, A. B., Johansen, T. H., Bratsberg H., Skjeltorp, A. T. (1993). *Physica C,* Vol.218, Issue 3-4, pp. 489-494, DOI: 10.1016/0921-4534(93)90055-U.
Riise, A. B., Johansen, T. H., Bratsberg, H., Koblischka, M. R., Shen, Y. Q. (1999). *Physical Review B (Condensed Matter and Materials Physics,* Vol.60, Issue 13, pp.9855-9861, DOI:10.1103/PhysRevB.60.9855 .
Riise,A.B., Johansen, T. H., Bratsberg, H., Koblischka, M. R. & Shen, Y. Q. (1999). *Phys. Rev. Lett. B*, Vol.60, pp. 9855.
Sanchez A. & Navau C. (2001). *Physica C*, Vol.360, pp. 364–365.

Sanchez, A. & Navau, C. (1997). *Physica C,* Vol.275, pp. 322.
Sanchez, A., Del Valle, N., Pardo, E., Chen, Du-Xing, & Navau C. (2006). Magnetic levitation of superconducting bars, *J. Appl. Phys.* Vol.99, pp. 113904 DOI:10.1063/1.2201767.
Schonhuber, P. & Moon, F.C. (1994). Levitation forces, stiffness and force-creep in YBCO high-tc superconducting thin films, *Applied superconductivity*, Vol.2(7/8), pp. 523-534.
Takao, T., Kameyama, S., Doi, T., Tanoue, N. & Kamijo, H. (2011). Increase of Levitation Properties on Magnetic Levitation System Using Magnetic Shielding Effect of GdBCO Bulk Superconductor, *IEEE Transactions On Applied Superconductivity*, Vol. 21, No.3, pp. 1543-1546.
Torng, T. & Chen, Q. Y. (1992). J. Appl. Phys., Vol.73, pp. 1198.
Tsuchimoto, M., Takeuchi, H. & Honma, T. (1994). *Trans. IEE of Japan* Vol.114-D, pp. 741.
Vandevelde, L., Melkebeek, J.A.A. (2001). A survey of magnetic force distributions based on different magnetization models and on the virtual work principle, *Magnetics, IEEE Transactions on,* Vol.37 Issue: 5, pp. 3405 – 3409.
Weber, H. W. (2001). Pinning F., *in Handbook on the Chemistry and Physics of Rare Earths*, Vol. 31: High Temperature Superconductors – II, ed. by K. A. Gschneider, Jr., L. Eyring, M. B. Maple (Elsevier, Amsterdam, 2001) pp. 187.
Wei, J.C., & Yang, T.J. (1996). *Chin. J. Phys.,* Vol.34, pp. 1344.
Xu, M., Shi, D., & Fox, R. F. (1990). Generalized critical-state model for hard superconductors, *Phys. Rev. B*, Vol. 42, pp. 10773-10776.
Yang, W.M. (2001). *Physica C,* Vol.354, pp. 5.
Yang, W.M., Zhou, L., Feng, Y., Zhang, P.X., Nicolsky, R. & de Andrade Jr, R. (2003). *Physica C,* Vol.398, pp. 141.
Yanmaz, E., Balci, S. & Küçükömeroğlu, T. (2002). *Materials Letters* Vol.54, pp. 191.
Yin, D., Schauer, W., Windte, V., Kuepfer, H., Zhang S. & Chen. J. (1994). *Z. Phys.*, B94, pp. 249.
Yin, D., Schauer, W., Windte, V., Kuepfer, H., Zhang, S., & Chen, J. (1994). A new understanding of the resistive state and the V-I characteristic of High-Tc superconductors, *Z. Phys. B,* Vol.94, pp. 249-254.
Yoshida, K., Sano, Y., & Tomii, Y. (1995). *Supercond. Sci. Technol.*, Vol.8, pp. 329.
Zhao X.F. & Liu Y. (2007). *J. Low Temp Phys.,* Vol.149, pp. 200.

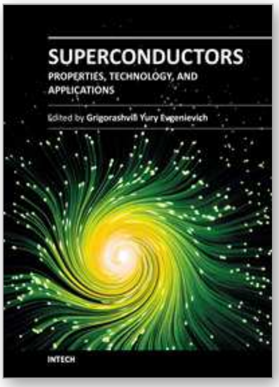

Superconductors - Properties, Technology, and Applications
Edited by Dr. Yury Grigorashvili

ISBN 978-953-51-0545-9
Hard cover, 436 pages
Publisher InTech
Published online 20, April, 2012
Published in print edition April, 2012